Combined X-ray Absorption Spectroscopy and Density Functional Theory Examination of Ferrocene-Labeled Peptides

R. G. Wilks* and J. B. MacNaughton

Department of Physics and Engineering Physics, University of Saskatchewan, 116 Science Place, Saskatoon, Saskatchewan, S7N 5E2, Canada

H.-B. Kraatz

Department of Chemistry, University of Saskatchewan, 110 Science Place, Saskatoon, Saskatchewan, S7N 5C9, Canada

T. Regier

Canadian Light Source Incorporated, University of Saskatchewan, 101 Perimeter Road, Saskatoon, Saskatchewan, S7N 0X4, Canada

A. Moewes

Department of Physics and Engineering Physics, University of Saskatchewan, 116 Science Place, Saskatoon, Saskatchewan, S7N 5E2, Canada

Received: November 14, 2005; In Final Form: January 27, 2006

A combination of soft X-ray absorption spectroscopy (XAS) measurements and StoBe density functional theory (DFT) calculations has been used to study the electronic structures of the ferrocene-labeled peptides Fc-Pro$_n$-OBz ($n = 1-4$). Excellent agreement between the measured and the simulated data is observed in all cases, and the origin of all major spectral features was assigned. The breaking of the degeneracy of the ferrocene $3e_{2u}$-like unoccupied molecular orbital under the influence of a substituent attached to a Cp ring was observed experimentally. The influence of the bonding environment on the O 1s and N 1s XAS spectra was examined. A corrected assignment of one of the major features in the Fe 2p XAS spectra of ferrocene is proposed and supported by the DFT simulations, as well as the measured spectra.

Introduction

Spectroscopic methods have been used in the past to study the electronic structure of ferrocene (Fc),[1−5] with the goal of mapping its unoccupied density of electronic states. This structure is related to the molecule's electronic properties and has an impact on the emerging field of molecular electronics, as it was shown in a recent study (not involving spectroscopy) that a particular ferrocene-containing molecular wire exhibits nearly perfect conduction of electrons.[6] In this publication, we present the results of a study of similar materials, namely, helical peptides that have been modified by the attachment of electroactive ferrocene carboxylic acid (Fc-COOH) and benzyl ester moieties. This study is the first known attempt to provide a combined theoretical and experimental spectroscopic examination of modified peptidic materials and is the only such study of ferrocene molecules that have been modified by the attachment of substituents of sizes comparable to the Fc itself. The study of peptides and their interaction with attached structures is vital to the understanding of the behavior of peptides in larger materials, such as proteins. In addition, understanding the electronic structure of peptides will aid in the design of novel materials, tailored to exhibit particular properties.

A number of recent studies has been focused on understanding the electronic structures of amino acids and peptides. Originally, these studies were motivated by a desire to use the spectra of the amino acids to identify the presence of particular acids in proteins. To this end, Boese et al. measured the C 1s XAS spectra of six common amino acids, as well as four dipeptides and a tripeptide.[7] Using a building block approach, they determined that the C 1s XAS spectra of the peptides was well-represented by the sum of the spectra of the appropriate amino acid monomers; the peptide bond was shown to have little effect on the electronic structure of the carbon sites. This result was supported by the spectral simulations performed by Carravetta et al.,[8] which employed site-specific spectral analysis, a technique that is utilized in the current study. Kaznacheev et al. expanded the database of C 1s XAS spectra of amino acids, recording the spectra of 19 different monomers,[9] including proline (Pro), which is the subject of this study. Our work confirms that the C 1s XAS spectra of peptides can be, for the most part, modeled using a building block approach, but the study is extended to include an examination of the O 1s and N 1s XAS of the peptides, as well as the effects of the interaction of the peptide with electroactive moieties. It is clear from our results that these effects have a significant influence on the electronic structures of the N and O sites, which may be more promising probes of protein electronic structure, given that they are much less common in such structures than are C atoms.

* Corresponding author. Tel.: (306)966-6380; fax: (306)966-6400; e-mail: regan.wilks@usask.ca.

10.1021/jp056573l CCC: $33.50
Published on Web 03/04/2006

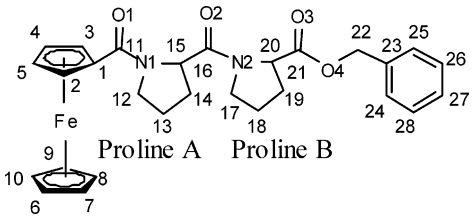

Figure 1. Structure of Fc-Pro$_2$-OBz, showing the numbering scheme of the atoms.

With the exception of Tanaka et al., who measured and simulated the O 1s XAS spectra of several amino acids,[10] and Tzvetkov et al., who used C 1s and O 1s XAS to study the adsorption of glycine on an oxide surface,[11] all of the groups that measured more than only the C 1s edge examined all three relevant absorption edges. Gordon and Cooper et al. focused largely on the spectra of glycine and glycine peptides, performing XAS measurements and complementary Hartree−Fock simulations to analyze the effects of the conformation of the peptides on their spectra.[12,13] Their observations highlight the need for accurate representations of the true structure of a molecule in electronic structure calculations; the structures obtained from previously published X-ray diffraction data[14] are used in our study. Plashkevych et al. also compared simulations with measurements, extending the work to include circular dichroism measurements.[15,16] Their conclusion that N 1s XAS spectra could be quite useful in differentiating between various amino acids reflects the sensitivity of these sites to their chemical environment. This theme is explored in detail in our study, as it is shown that the N 1s XAS spectra are influenced by the extended environment, leading to differences in the spectra associated with the various sites in a peptide of a single amino acid (proline). Further evidence of the sensitivity of the N electronic structure to its environment is provided by Messer et al., who showed significant changes in the N 1s XAS spectra of glycine, diglycine, and proline in solution, as a function of the solution's pH.[17,18]

The work of Nyberg and Hasselström involves the measurement and simulation of all three relevant absorption edges in glycine adsorbed onto substrates,[19−22] using StoBe DFT to perform the simulation. In addition to producing a large database of the C, N, and O XAS spectra of 22 amino acids,[23] Zubavichus et al. clearly documented the effects of radiation damage on the XAS spectra of amino acids, showing that, in general, the spectral features became broader and less distinct as a result of damage by soft X-rays.[24,25] Their study shows that radiation damage must be taken into account in any study of amino acid spectra; it will be shown later that it had, at most, a negligible effect on the current study.

The details of the structures and synthesis of the compounds in this study have been described in detail in previous publications.[14,26] In general, a proline peptide is modified by the attachment of a moiety of Fc-COOH to its N-terminus and a benzyl ester to its C-terminus. The resulting series of compounds is referred to as Fc-Pro$_n$-OBz ($n = 1-4$). A diagram of Fc-Pro$_2$-OBz is shown in Figure 1; the numbering scheme will be employed in the discussion of the calculated XAS spectra that are a main topic of this paper. The study of these particular peptides is motivated by their unusual electrochemical properties, which have been observed in cyclic voltammetry (CV) experiments. It was observed that the redox potential of the Fc-Pro$_n$-OBz series decreased as the number of residues was increased, up to the addition of the third proline.[14] This behavior is contrary to the expected relationship because it is expected that the distance between the electron donor (ferrocene) and the acceptor (benzene) will increase with each residue that is added to the peptide. The mechanisms governing molecular electron transfer in general are poorly understood, despite playing an important role in many biological processes. It is felt that if the anomalous behavior seen in the Fc-Pro$_n$-OBz molecules can be understood, insight into the mechanisms governing electron transfer in peptides and proteins can be obtained. Our study has produced a great deal of information about the electronic structure of the organometallic materials in question, and it illustrates the usefulness of site-selective density functional theory calculations in the analysis of the X-ray absorption spectra of complicated molecules. This technique has proven to be extremely useful in similar studies of smaller molecules.[8,27]

Experimental Procedures and Calculations

All elements in Fc-Pro$_2$-OBz were examined using XAS, recorded in the total electron yield (TEY) mode. The 1s absorption edges of C, N, and O were probed, along with the 2p absorption edge of Fe. XAS is governed by standard dipole selection rules, and so excitation of these core levels probes the low-lying unoccupied states having p-type symmetry (for 1s excitation) or s- and d-type symmetries (for 2p excitation). The N and O 1s XAS spectra in this study were measured at beamline 6.3.2.1 at the Advanced Light Source (ALS) synchrotron at Lawrence Berkeley National Laboratory. Beamline 6.3.2.1 is a bending magnet beamline giving high resolution in the soft X-ray region; the details of the beamline are discussed elsewhere.[28,29] For this study, a bending magnet source was preferable to an undulator source because the significantly higher intensity of the latter device would cause significant radiation damage to the sample being measured.[24,25]

The C 1s and Fe 2p XAS spectra were measured at the spherical grating monochromator (SGM) beamline at the Canadian light source (CLS) synchrotron at the University of Saskatchewan. The details of this beamline will be discussed in a forthcoming publication. Although it is an undulator beamline, radiation damage was not an issue at this point because the low ring current that was used at the facility (30−50 mA; necessary for the conditioning of the vacuum during commissioning) at the time of these measurements were performed limited the amount of photons that are incident on the sample. Several of the spectra obtained at beamline 6.3.2.1 were remeasured at the CLS to establish the reproducibility of the experiment. In addition, several new spectra were measured at the SGM beamline to support and clarify some of the analysis of the spectra from beamline 6.3.2.1. In terms of normalization of the measured spectra, the SGM beamline has an advantage because it allows the incoming photon flux to be measured (via a highly transparent gold mesh) simultaneously with the spectrum. The flux measurement for normalization of the N 1s XAS measurement, performed at beamline 6.3.2.1, was performed by taking a subsequent measurement of clean indium foil. Because oxygen contamination of the foil could not be removed, these spectra were normalized to a current measured from one of the mirrors. The C, N, and O 1s XAS spectra were recorded with a resolution of approximately 0.1 eV, while Fe 2p XAS had a resolution of approximately 0.2 eV.

Proper preparation of the samples for measurement is a key component of XAS experiments on organic materials. In this study, a solution was made of the powdered samples using ethyl alcohol. The solution was painted onto indium foil, where the alcohol evaporated quickly. This procedure is similar to that used by Kaznacheev et al. in their study of various amino acid

monomers.[30] In that study, it was found that preparing the samples in this way had little or no effect on their structure, a conclusion that is confirmed in this study. This method eliminates any effects due to sample charging, which can make the measurement and analysis of electron yields spectra quite difficult. Mounting the samples on indium foil also minimizes the possibility of carbon contamination, which, along with radiation damage, may have affected some of our previously reported measurements of these same samples.[31] The energy axes of the spectra were calibrated with respect the energies of peaks in the spectra of reference samples (HOPG for C 1s calibration,[32] h-BN for N 1s,[33] and TiO_2 for O 1s[34]). The exception to this procedure was the Fe 2p XAS spectra, where the main resonant feature was assumed to occur at the same energy as the previously reported results for gaseous ferrocene.[1]

Simulations of the XAS spectra of all elements in Fc-Pro_2-OBz were performed using the StoBe-deMon DFT software.[35] StoBe takes as input the *x*,*y*,*z* coordinates of the atomic sites (in units of angstroms in this case), as well as basis set and exchange/correlation potential information. The atomic coordinates of the heavy elements were obtained from the X-ray diffraction data;[36] the hydrogen sites needed to be added in afterward. The exception was the O3 site, which is part of the carbonyl group at the C-terminus of the peptide. The length of the bond between this oxygen and the adjacent carbon was 1.16 Å, approximately 10% shorter than the other two carbonyls. The resulting spectral simulations were inconsistent with the measured results, suggesting that the large amount of thermal noise observed in the X-ray diffraction patterns associated with this portion of the molecule may have led to an error in the length of the bond. It is also possible that the disagreement represents a difference in structure between the crystalline structure and the structure of the dried solutions measured in this study. Whatever the cause, when the bond length was changed to 1.26 Å (the average of the other two carbonyl bond lengths), the agreement was much improved, and it is these results that are presented in the O 1s XAS section. The only other geometry optimization that was performed was done to position the hydrogen atoms while the other atoms were fixed in place.

This study uses triple-ζ plus valence polarization (TZVP) Huzinaga orbital basis sets and A5 auxiliary basis sets derived from the TZVP basis sets.[37] The orbitals of the atom undergoing excitation were represented by an iii_iglo basis set,[37,38] and a large, diffuse auxiliary basis set was added at this location to model the unoccupied orbitals. StoBe model XAS spectra use a transition state approximation, in which an electron in the core level that is undergoing excitation (i.e., a C 1s electron) is replaced by a half-occupied core hole. The orbitals are then calculated in this excited state, and the transition probabilities between the core state and all of the unoccupied states in this excited configuration are then determined. To model the Fe XAS spectrum, slight adjustments to the previous procedure were necessary. Rather than place the half core hole in a particular $2p_{3/2}$ orbital, it was spread evenly across all three core orbitals (i.e., each orbital was given an occupation of $0.8\bar{3}$). This enforces a condition of degeneracy on the core orbitals, and it was found to be the only way to avoid convergence-inhibiting oscillations in the SCF procedure.

To ensure that the half-occupied core hole was localized on a particular atomic site, all other atoms of that same element were represented by pseudopotentials, where the nucleus and innermost electrons are replaced by a single point charge, corresponding to the sum of the individual charges. Special basis sets were employed to ensure that the remaining electrons accurately represent the higher-lying electrons of the atom. This procedure was, of course, only necessary for the calculations of the C, N, and O 1s XAS spectra, as there is only one Fe atom in the structure. As a result of the need for pseudopotentials in the calculations, the spectrum associated with each site in the molecule needed to be calculated separately. This procedure of calculating site-resolved XAS spectra facilitated an examination of transitions that would otherwise have been overwhelmed by larger features in the spectrum. The C 1s XAS spectrum of Fc-Pro_2-OBz is composed of the superposition of 28 nonequivalent carbon spectra. While the sum of the calculated spectra provides a very good reproduction of the experimental data (Figure 6, discussed in the following section), the site-resolved spectra essentially represent a deconvolution of the measured spectrum into 28 components. This representation allows for a great deal of flexibility in analysis.

Although the compounds in this study do not belong to a common point group, it is convenient to make use of a traditional labeling scheme to describe the various molecular orbitals of the system, rather than the generic system (i.e., labeling the orbitals 1A, 2A, 3A, etc.) that is mathematically correct. Therefore, the orbitals associated with a particular component (i.e., the ferrocene) will be described in terms of the isolated molecule. Thus, the discussion will contain references to $4e_{1g}$-like and π^* orbitals, although these labels are not consistent with the symmetry of the actual system under consideration. The ferrocene labels correspond to the D_{5d} configuration of free ferrocene.

Results and Discussion

The following sections describe the results of the XAS measurements that were performed at beamline 6.3.2.1 at the ALS and at the SGM beamline at the CLS. Attempts were made to determine what effect, if any, radiation damage had on the samples. To this end, after several of the XAS spectra were measured, a second XAS spectrum was measured immediately afterward on the same spot, with the excitation energy decreasing iteratively, rather than increasing. This ensured that the subsequent measurements of the low-energy features, which were observed to vary strongly as a function of radiation dose,[24,25] were separated by approximately 7 min. As radiation damage was previously shown to be a cumulative effect,[24,25] any change in the shape of the prominent low energy features would be maximized by this procedure. No variation in the shapes of these features was observed in any spectrum, and so it was assumed that the effects of radiation damage on the XAS spectra were negligible. As further confirmation of this assumption, all samples were intentionally damaged by bombardment with high levels of radiation. The general appearance of the spectra of the damaged samples matched the observations of Zubavichus et al. To further ensure that radiation damage was held to a minimum, the exposure time before data collection was kept as small as possible, and a new spot on the sample was chosen for each measurement.

C 1s XAS. Figure 2 shows the C 1s XAS spectra of the series Fc-Pro_n-OBz ($n = 1-4$), measured at the CLS. The locations of the major spectral features are marked with arrows. The preedge features in Figure 2 (and Figure 3) are indicative of varying degrees of sample charging. The variations are exaggerated by the normalization procedure, which consisted of assigning a minimum sample current of zero to each spectrum, then scaling them to a common value at feature a. Feature a is centered at approximately 285.5 eV. As can be deduced from

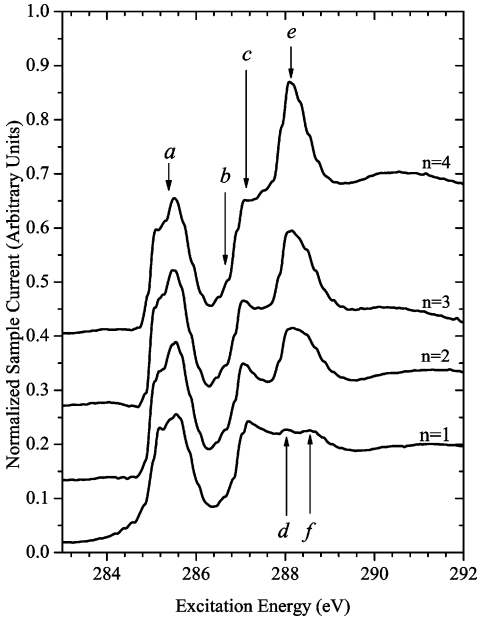

Figure 2. C 1s XAS spectra of the series Fc-Pro$_n$-OBz. A uniform background signal has been subtracted from all spectra, and the magnitudes of the sample currents were normalized at feature a. A vertical offset has been added for clarity.

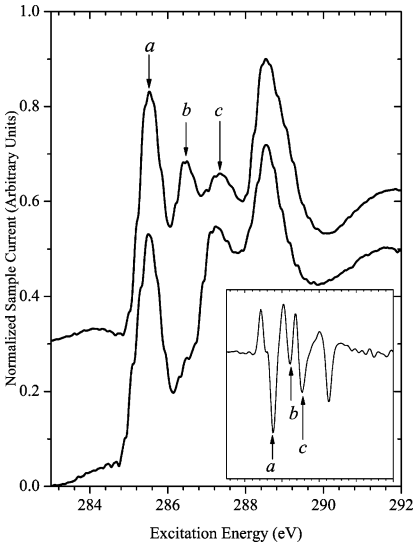

Figure 3. C 1s XAS of Fc-COOH (bottom) and the 1,*n*′-disubstituted Fc-(COOH)$_2$. Both spectra have had a uniform background subtracted and had the value of the sample current normalized at the location of feature a. A vertical offset has been added for clarity. The inset shows the second derivative of the (smoothed) Fc-COOH spectrum, with the locations of the relevant features indicated. The energy scale of the inset is the same as that of the main panel.

its appearance, this prominent feature is comprised of the superposition of a number of transitions. Comparison to previously published studies suggests that feature a has significant contributions from both a benzene π^* feature[39] (~285.3 eV) and a ferrocene 4e$_{1g}$-like feature[3] (~285.6 eV). The ferrocene 4e$_{1g}$ orbital is largely associated with the lowest unoccupied Fe 3d orbitals. Because each molecule in the series Fc-Pro$_n$-OBz contains a single ferrocene and a single benzyl ester, it was assumed that the shape of this feature would not change significantly. The four spectra were therefore normalized such that they had the same value of the sample current at 285.5 eV.

Feature c resembles a peak seen in previous studies of ferrocene (and substituted ferrocenes) and can be assigned to transitions into a ferrocene 3e$_{2u}$-like orbital.[3] The 3e$_{2u}$ orbitals are the lowest unoccupied orbitals associated with the cyclopentadienyl (Cp) ligands of the ferrocene. The ratio of the intensity of this feature to that of feature a remains fairly constant, supporting its association with a ferrocene-related orbital. Features d−f are assigned to transitions into π^* orbitals associated with the various carbonyl groups of the peptide.[30] These orbitals do not occur at the same energy, due to the differences in the environment of the carbonyl groups. The intensity of feature e increases as a function of the number of proline residues in the peptide, suggesting that it is associated with the carbonyl groups located at the interproline bonds. This assumption is further justified by the feature's absence from the spectrum of Fc-Pro-OBz, which has no interproline bond. The two carbonyl groups in Fc-Pro-OBz are located in dissimilar environments; one is adjacent to the ferrocene, attached to the N-terminus of the peptide, and the other forms the C-terminus of the peptide, to which the benzyl ester is attached via a single C−O bond. It is expected that the π^* orbitals of these two groups would be found at different energies, as it has been shown that the energy positions of transitions into such states increase as the electronegativity of the surrounding environment increases.[40] Because the C-terminus of the peptide is expected to be more electronegative than the N-terminus, feature f is associated with the carbonyl group at the first location, while feature d is assumed to be associated with the latter. Both of these features are present as shoulders in the spectra of the larger peptides.

The origin of feature b cannot be determined by simply examining previously published spectra. It is proposed that this feature can be attributed to a splitting of the ferrocene 3e$_{2u}$-like orbitals under the influence of the substituent. This splitting is expected to occur but was not observed in previous studies, which used lower-resolution electron energy loss spectroscopy (EELS) techniques.[1,4] Evidence in support of this assignment can be seen in the C 1s spectra of ferrocene carboxylic acid and the 1,*n*′-disubstituted Fc-(COOH)$_2$, shown in Figure 3. The inset of Figure 3 shows the second derivative of the Fc-COOH spectrum and is intended to clarify the position of feature b, which may not be clear from the spectra in Figures 2 and 3. The most obvious differences between the spectra are seen in the relative intensities of features b and c, which are found at the same energies as in the spectra of Fc-Pro$_n$-OBz (Figure 2). The shape of this portion of the spectrum of Fc-COOH is quite similar to those shown in Figure 1, suggesting that the assumption of a ferrocene-based final state is a valid one. The spectrum of Fc-(COOH)$_2$, however, is radically different in this area, suggesting that there is a significant effect of the substituent on the orbital. In this spectrum, feature b is more intense than feature c, suggesting that its final state is closely associated either with the substituted cyclopentadienyl ring or with the substituent itself. In addition to the information about features b and c, the proposed origin of the prominent feature a is confirmed by the spectra in Figure 3. It would be expected that this feature would differ slightly from the comparable features in the previous figure because Fc-COOH and Fc-(COOH)$_2$ do not contain a benzyl ester. The spectra show that this is exactly the case and that feature a is at the same energy (285.6 eV) as the features attributed to transitions into 4e$_{1g}$-like orbitals in the discussion of the spectra in Figure 2.

The site-resolved C 1s XAS spectra of the two cyclopentadienyl rings (Cp′ and Cp denoting the substituted and unsubstituted rings of the ferrocene, respectively) and the benzyl ester of Fc-Pro$_2$−OBz that were simulated using StoBe are shown

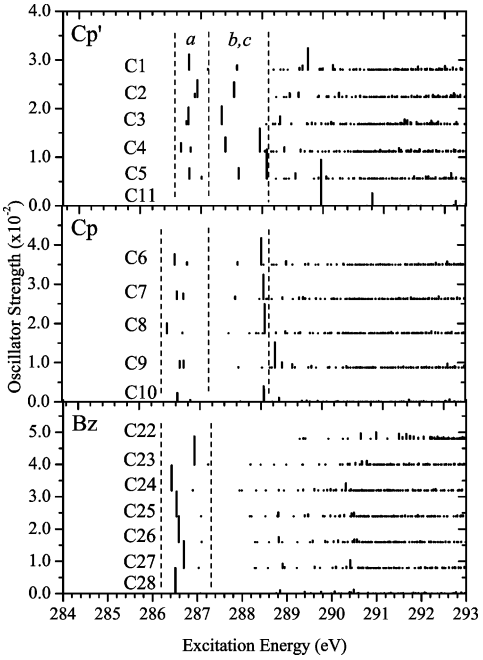

Figure 4. Simulated C 1s XAS of the individual sites in the substituted Cp ring (Cp′, top panel), unsubstituted Cp, and benzene ring in Fc-Pro_2-OBz. The energy regions corresponding to features a−c in Figures 2 and 3 are indicated, with the boundaries marked with dashed vertical lines. All spectra have had a vertical offset added for clarity.

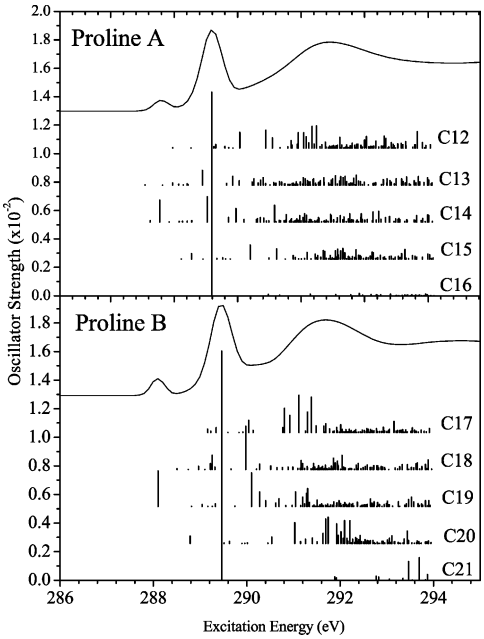

Figure 5. Simulated site-resolved C 1s XAS of the proline residues of Fc-Pro_2-OBz. The summation of the individual broadened spectra is displayed above the oscillator strengths.

in Figure 4. The spectra of the proline sites are not included in Figure 4; they are displayed separately in Figure 5. The energy axes of all of the simulated spectra are displayed as calculated; an energy shift will later be applied to align them with the experimental results. The exception is in the spectra of the three carbonyl sites shown in Figures 4 and 5 (C11, C16, and C21), which were shifted by different amounts to agree with the location of the corresponding peaks in the measured spectrum. The analysis of these spectra is complicated by the fact that convergence of the SCF procedure could not be achieved using the same parameters as in the simulations of the other spectra, and so the energy axes were not necessarily comparable. The π^* peaks in the spectra of the carbonyls C11 and C16 were found at the same energy, but this is contradicted by the measured spectra. Because these two spectra were calculated using a number of different parameters, including different basis sets, it will be assumed that the energies observed in the measured spectra were correct and that the two π^* peaks are not, in fact, found at the same energy. The calculation of the C-terminus carbonyl, C21, was particularly difficult, and the convergence could not be achieved until the ferrocene moiety was removed from the model completely. As the interaction between the peptide and the moiety is one of the foci of this study, the spectrum of C21 is included merely for completeness, having been shifted to correspond to the location of feature f in the measured C 1s XAS spectrum, which was assigned, with a great deal of confidence, to the π^* peak of this particular carbonyl. Regrettably, no analysis of the carbonyl C 1s XAS spectra can reliably be performed.

The origin of feature a in Figure 2 is confirmed by the calculations, as it is clear that this energy region is dominated by transitions that are localized on the ferrocene and benzene sites. Although the peaks are seen at several different energies in the various spectra, examination of the StoBe output files shows that they are the result of transitions into only four nondegenerate orbitals, two each on the ferrocene and benzene. The differences in the transition energies arise from variations in the calculated transition-state energy levels of the respective C 1s core levels. The two lowest-energy peaks in the ferrocene spectra are attributed to $4e_{1g}$-like orbitals. The two orbitals are nondegenerate, and Figure 4 provides an indication that, even if the experimental resolution could be drastically improved, the splitting between the features could not be observed, due to the differences in transition energy brought about by the shifts in the C 1s levels of the various carbon sites. These differences also complicate the analysis of the calculated spectra, as transitions into a common orbital do not form a single peak. To analyze the site-specific spectra, the term values ($E_{core} - h\upsilon_{exc}$), which indicate the energy of the destination orbital relative to the continuum, are calculated. Table 1 shows the average values of the core energy and peak position ($h\upsilon_{exc}$), as well as the proposed final orbital of several of the C 1s XAS transitions seen in Figure 4. The spread of the values contributing to the average is indicated by the ± value next to the energy. The values given correspond to the peak locations in the simulated spectra as they were calculated, not taking into account the −1.2 eV shift that must be applied to all spectra to align them with the measured spectrum. The energies E_{core} are obtained from the StoBe output files and correspond to the calculated energies of the half-occupied core holes used in the simulations of the XAS spectra.

Continuing along the energy scale, the next two ferrocene orbitals are found at the same energies as features b and c in Figures 2 and 3. The character of these peaks differs from that of the $4e_{1g}$-like orbitals, in that each is largely associated with a particular cyclopentadienyl ring. Specifically, the peaks corresponding in energy to feature b are found mostly on the substituted ring Cp′, while the peaks corresponding to feature c are found on the unsubstituted ring Cp. The transitions from the Cp′ core states to the Cp orbitals are considered separately, as they are, in general, less prominent and react differently to the presence of the core hole. The $3e_{2u}$-like orbital associated with the Cp′ ring is found at lower energy than the corresponding Cp orbital, due to the stabilizing effects of the substituent. The association of the final states with a specific ring supports the

TABLE 1: Transition Energies and Term Values of Features in Simulated C 1s XAS Spectra

sites	core level[a] (eV)	feature[a] (eV)	term value[a] (eV)	assignment (feat.)
		Ferrocene sites		
C1−10	290.96 ± 0.28	286.66 ± 0.30	4.30 ± 0.10	$4e_{1g}$-like (a)
C1−10	290.96 ± 0.28	286.88 ± 0.28	4.08 ± 0.14	$4e_{1g}$-like (a)
C1−5	291.05 ± 0.17	287.73 ± 0.19	3.32 ± 0.09	$3e_{2u}$-like #1 (b)
C6,7,8,10	290.83 ± 0.13	287.93 ± 0.06	2.97 ± 0.04	$3e_{2u}$-like #1 (b)
C6,7,8,10	290.83 ± 0.13	288.46 ± 0.05	2.42 ± 0.04	$3e_{2u}$-like #2 (c)
C1−3,8,9	290.99 ± 0.28	288.89 ± 0.38	2.14 ± 0.02	C−H σ*
C1−10	290.96 ± 0.28	289.00 ± 0.41	1.95 ± 0.10	C−H σ*
		Proline sites		
C14	291.32	287.93	3.39	N−H σ* B (minor)
C14	291.32	288.13	3.19	N−H A σ*
C15	292.14	288.60	3.55	N−H σ* B (minor)
C15	292.14	288.81	3.32	N−H σ* A
C19	291.86	288.10	3.76	N−H σ* B
C20	292.65	288.79	3.86	N−H σ* B
		Benzene sites		
C23−28	291.10 ± 0.21	286.61 ± 0.26	4.49 ± 0.07	C=C π* (*a*)
C23−28	291.10 ± 0.21	287.07 ± 0.17	4.03 ± 0.09	C=C π* (*a*)
C23−28	291.10 ± 0.21	289.46 ± 0.24	1.64 ± 0.09	π* b_{2g} + Rydberg[b]

[a] Average value for all sites involved in transition. [b] Assignments based on those given by Püttner et al.[41] for benzene.

previous assignment of these peaks to transitions into $3e_{2u}$-like orbitals. A possible explanation for this ring specificity, in contrast to the $4e_{1g}$-like orbitals, lies in the close association of the former orbitals with the C π* orbitals of the Cp rings, as opposed to the latter orbitals, which have more of an Fe 3d character. It seems likely that any effect that the presence of the substituent may have on the Fe atom in the ferrocene (specifically leading to a break in the degeneracy of orbitals) would be reflected in its interaction with the unsubstituted Cp ring, while the effect of the substituent on the C π* orbitals would be more localized.

The contributions of the benzyl ester site to feature a are also seen clearly in Figure 4. The lowest-energy transitions are associated with π* orbitals[42] and are observed only on the sites associated with the benzene ring, not on the substituent carbon. Close examination reveals that several spectra have a low intensity feature ~0.4 eV above the main resonance. It is suggested that this feature may be due to dipole-forbidden transitions into the a_2 orbital that is formed when the degeneracy of the main benzene e_{2u} (π*) orbital is broken as a result of the reduction of symmetry that is caused by the presence of the core hole[43] and the substituent.

Figure 5 shows the site-resolved simulation of the C 1s XAS spectra of the two proline residues of Fc-Pro_2-OBz. Proline A is the residue proximal to the ferrocene moiety, and proline B is the distal residue. Note that the energy axis in Figure 5 is not equivalent to that in the other figures showing C 1s XAS spectra, although the magnitude of the range is equivalent. The spectra are dominated by the intense transition into the carbonyl π* orbitals. The other distinct feature that is seen in both spectra in Figure 5 occurs at slightly above 288 eV (energy as calculated, without the −1.2 eV shift applied). These features have term values of 3.19 eV (site C14) and 3.76 eV (site C19) and are also seen, at a slightly higher energy, in the spectra of the α-carbon sites C15 and C20. These features do not involve the same unoccupied orbitals; the proline B transitions involve the same destination orbital as in the minor transition seen at slightly lower energy in the proline A simulations. The peak positions and term values of these transitions are given in Table 1. These C 1s XAS features are closely linked to features in the N 1s XAS spectra and are assumed to have an origin stemming from the N−C σ* orbitals. When shifted, these features will be found at approximately 286.8 eV, suggesting

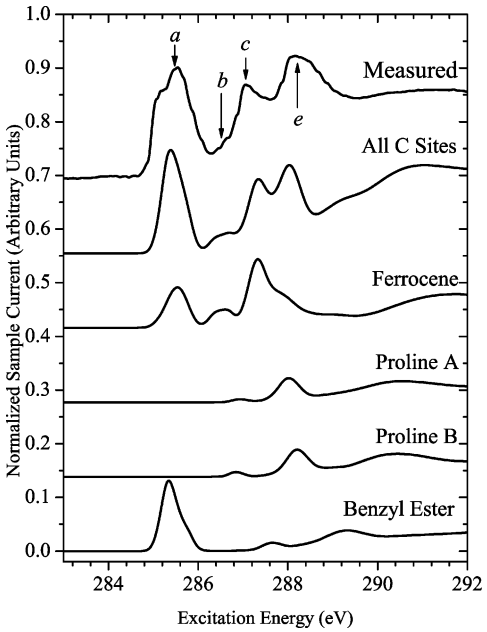

Figure 6. Simulated C 1s XAS spectrum of Fc-Pro_2-OBz as compared to the measured spectrum. The component-resolved C 1s XAS spectra are also included. A vertical offset has been added for clarity.

that feature b in the measured C 1s XAS in Figure 2 has a contribution from the peptide. This contribution can be seen more clearly in Figure 6.

Summation of the individual spectra of all of the C sites in the molecule provides a representation of the measured spectrum. Figure 6 shows the close agreement between the Fc-Pro_2-OBz spectrum measured at the CLS and the StoBe DFT simulation. Also included in the figure are the summations of the C sites of each individual component in the compound. The energy axes of all spectra have been shifted 1.2 eV to lower energy to correspond to the measured spectrum. The exceptions to this are, of course, the contributions from the carbonyl sites, which were discussed earlier. A nonuniform Gaussian broadening scheme was applied to the individual spectra prior to summation to provide a more realistic model of the measured spectrum, one that attempts to account for instrumental and lifetime broadening. Below 286.8 eV, the spectra were convoluted with a Gaussian of width 0.3 eV, and above 315 eV, they

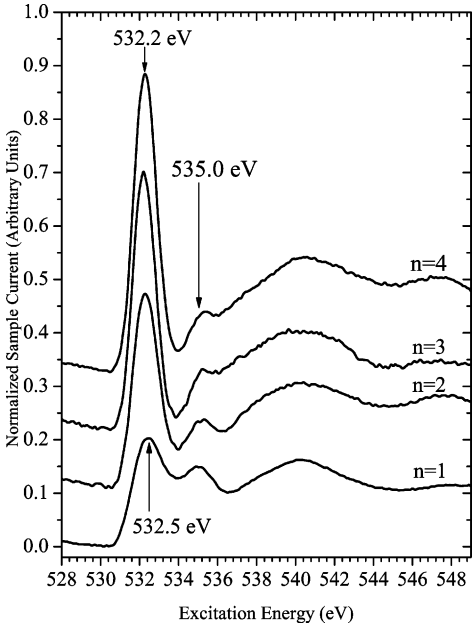

Figure 7. O 1s XAS of the series Fc-Pro$_n$-OBz. All spectra have had a uniform background subtracted, and a vertical offset has been added for clarity.

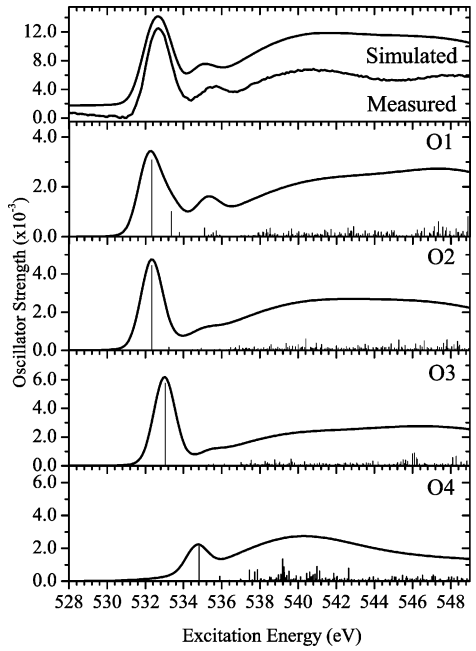

Figure 8. Simulated O 1s XAS spectra of the individual oxygen sites in Fc-Pro$_2$-OBz. The summation of the four spectra is compared to the measured spectrum in the top panel. A vertical offset was added to the simulated spectrum for clarity.

were convoluted with a much broader Gaussian function (6.0 eV), in an attempt to reproduce this largely featureless portion of the spectrum. Between the two regions described previously, the width of the Gaussian was varied linearly between the values at the boundaries.

O 1s XAS. The O1s spectra of the Fc-Pro$_n$-OBz series are shown in Figure 7. The minimum value of all spectra has been set to zero, and they were then normalized to the intensity of the broad resonance feature located at approximately 539 eV. The sloping onset observed in the O 1s XAS spectra is evidence of a small amount of sample charging during the measurement. The O 1s XAS spectra in Figure 7 are dominated by the feature centered at 532.2 eV, with the exception of the Fc-Pro-OBz spectrum, in which the main peak is located at 532.5 eV. The 532.2 eV peak is associated with transitions into the carbonyl π^* orbitals located at the interproline bonds. Previous publications have shown that, as in the C 1s XAS, the environment of the carbonyl group cannot be neglected when the O 1s XAS spectra are being analyzed. Zubavichus et al. recently reported a shift of +0.2 eV in the position of the π^* resonance in the spectrum of triglycine (a three-residue glycine peptide) as compared to the mono- and diglycine spectra.[44] This result is similar to those obtained by Gordon and Cooper et al., where the shift was observed immediately upon going from the monomer to the dimer (i.e., as soon as a peptide bond was formed).[12,13] These shifts are in keeping with the general behavior that is expected in carbonyls, as the π^* peak in the O 1s XAS is expected to shift in much the same way as the corresponding C 1s feature.[40] The fact that the π^* feature in Fc-Pro-OBz is found at a higher energy than in the larger peptides would seem to contradict what has been previously reported, except that the carbonyl groups in the Fc-Pro-OBz sample are not found in the same environment as in the monomer, due to the presence of the Fc and the benzyl ester. In contrast with the other spectra in Figure 7, the main peak in the Fc-Pro-OBz spectrum is broad and flat, suggesting that it is composed of the superposition of more than one feature. Because the position of the O 1s π^* peak changes in the same way as the equivalent peak in the C 1s XAS, it is assumed that the resonance associated with the ferrocene carbonyl is found at a lower energy than the resonance associated with the C-terminus of the peptide.

The smaller feature at 535.0 eV is not seen in any of the previously reported peptide spectra, and so it can be assumed that it is not associated with the proline residues. It is a fair assumption that this feature is associated with the single-bonded oxygen site at the benzyl ester; it is comparable in energy to the feature observed by Tanaka et al. in the O 1s XAS spectrum of L-aspartic acid, attributed to the σ^* orbitals of a carboxyl group.[10] The simulated spectra shown in Figure 8 confirm that the feature in the measured spectra is associated with the benzyl ester oxygen site.

The simulated spectra in Figure 8 were convoluted with Gaussian functions of width 1.3 eV below 536.5 eV and width 6.5 eV above this energy. They were also shifted −0.4 eV to bring them into alignment with the measured spectrum. The term values and proposed assignments of the features seen in Figure 8 are displayed in Table 2. The calculated spectrum of O1 is dominated by the peak at 532.2 eV, with a secondary feature at 533.3 eV. These peaks are associated with transitions into the same orbitals as features a ($4e_{1g}$-like) and b ($3e_{2u}$-like) in the C 1s XAS spectra of the substituted Cp′, suggesting that these unoccupied orbitals make a significant contribution to the electronic structure of the substituent. The spectrum of O1 also exhibits a minor peak around 535.7 eV; a small shoulder in the measured XAS spectrum of Fc-Pro-OBz is found at this energy. This feature is composed of a number of minor transitions having term values around 0.85 eV, considerably lower than any of the other transitions discussed in detail in this manuscript. These transitions are presumably of σ^* character, although no unequivocal assignment can be made. The measurements of gas-phase glycine by Gordon and Cooper et al. show a distinct peak at this energy,[12,13] which was a result of the protonation of the carbonyl oxygen site. Kaznacheev et al. briefly examined the possibility that protonation in solid samples could be brought about by the ethanol used in the sample preparation; they concluded protonation is, at most, a minor effect.[30] The presence of the 535.7 eV feature in the simulated spectrum confirms that

the feature in Figure 7 is not due to protonation, verifying the previous results and justifying the model of the molecule that was used in the StoBe calculations.

Like the O1 spectrum, low-energy features dominate the simulated spectra of the O2 and O3 sites. As in the calculated C 1s XAS spectra associated with these two carbonyls, the peaks in the O1 and O2 spectra occur at the same energy. Comparison of the calculated carbon spectra with the experimental results suggested that the calculated peak was found at the wrong energy. The broadness of the main features in Figure 7 makes it impossible to determine whether the contributions from the two sites are found at the same energy in the experimental data, but examination of the output files for both spectra suggests that both transitions involve the same destination orbital. Because the energy of the O 1s orbital is not as sensitive to the environment as is the C 1s level, it is conceivable that the main peaks in the O1 and O2 spectra could be found at the same energy, while the corresponding peaks in the C 1s XAS are not. As this is what is suggested by the O 1s XAS calculations and the C 1s XAS measurement, both of which were successful, this will be assumed to be the case. The spectrum of the O3 site is also very simple, although the main resonance is shifted to a higher energy as compared to the O1 and O2 sites, reflecting the difference in the bonding environment of the O3 carbonyl. The main resonance is found at 533.6 eV; minor shoulders can be seen at this energy in the spectra shown in Figure 7. The spectrum of the benzyl ester oxygen site, O4, confirms the assignment of the 534.8 eV feature in Figure 7. The peak seen in the calculated spectrum is found at exactly this energy. The spectrum shows no evidence of any double-bonding character associated with the OBz oxygen.

N 1s XAS. The appearance of the features in the N 1s XAS spectra of amino acids and small peptides are extremely sensitive to the sample environment. Recent publications have shown that the characteristics of the N 1s spectrum of glycine, for example, change significantly depending on whether the sample is in solid or gaseous form,[12,13] adsorbed onto a substrate,[19,22] or in an aqueous solution.[17] Analyzing these spectra is much simpler than analyzing the C 1s XAS, due to the much smaller number of nonequivalent sites in the former spectra. In all cases, the molecules have a single N at the N-terminus of the peptide (bonded to the carbonyl group that is adjacent to the ferrocene) and a N atom at each interproline bond. The only exception is, of course, Fc-Pro-OBz, which has no interproline bond. Comparison of the spectrum of this smallest molecule allows the features that are seen in the spectra of the larger peptides to be assigned with greater ease.

The preedge intensity seen in the N 1s XAS spectra of Figure 9 is associated with small features in the indium normalization signal; no such features are seen in the region of interest. The lowest-energy transitions in the N spectra in Figure 9 are attributed to the partial π character of the nitrogen bonding.[7] Although all of the N sites in Fc-Pro$_n$-OBz are single-bonded to the three adjacent C atoms, the partial double-bond character arises from the overlap of the N orbitals with the carbonyl orbitals. Thus, all reported N 1s XAS spectra of peptides have a prominent peak in this energy range, while the spectra of amino acid monomers do not. Close examination of this feature shows that the center of the peak shifts from 401.7 eV in the spectrum of Fc-Pro-OBz to 402.2 eV in the spectra of Fc-Pro$_3$-OBz and Fc-Pro$_4$-OBz, with the Fc-Pro$_2$−OBz peak somewhere in the middle. This shift can be easily explained as being a result of the nonequivalence of the N sites in the molecules. It is clear that, although both represent N in an amide bond, the electronic

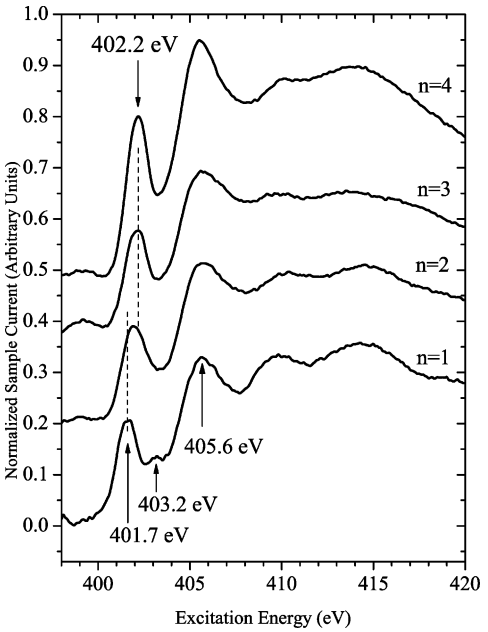

Figure 9. N 1s XAS of the series Fc-Pro$_n$-OBz. All spectra have had a uniform background signal subtracted, and the sample currents have been normalized at 401.7 eV. A vertical offset has been added for clarity.

structures of the N sites at the interproline bonds are different from the N-terminus of the peptide. Specifically, it seems that the presence of the ferrocene causes the final state of the N-terminus nitrogen site to be found at a lower-than-expected energy. This shift is not unexpected because the carbonyl orbitals that contribute to the π^* peak in the N 1s XAS spectrum are affected in this same way, as was discussed in the two previous sections.

The feature seen at 403.2 eV in the N 1s XAS spectrum of Fc-Pro-OBz is not seen in any previously published spectra of amino acids or peptides. Although it is not visible in the spectra of the larger peptides in Figure 9, it appears as a minor shoulder on the main π^* feature. Examination of the site-selective simulated spectra of Fc-Pro$_2$-OBz, however, provides a likely explanation of its origin. The plots in Figure 10 show the results of the StoBe simulation, including a minor feature at 403.3 eV in the spectrum of the N1 site, the peptide N-terminus. The term value of this transition is 1.92 eV, which is very close to that of the more prominent C−H σ^* transitions observed in the carbon spectra (see Table 1), suggesting a common origin.

Overall, the summation of the spectra of the two nonequivalent N sites provides an excellent representation of the measured spectrum. The calculated transitions were convoluted with Gaussians of width 0.9 eV below 403 eV, 3.5 eV above 408 eV, and linearly varying width between these two energies. The energy axes of the broadened spectra were then shifted downward by 0.4 eV to align them with the measured spectrum. The features at 402.9 eV in the simulated spectra correspond to a shoulder seen on the π^* peaks of the measured spectra of Fc-Pro$_n$-OBz ($n = 2-4$). The term values of these transitions are 3.08 eV for the N1 feature and 3.32 eV for the N2 feature, which are similar to that of the $3e_{2u}$-like orbital of the substituted Cp ring, suggesting that, as was seen in the calculated O 1s XAS spectrum of the nearby O1 site, this orbital may have a significant presence in the electronic structure of the substituent peptide. The output of the DFT calculations shows that both transitions involve the same unoccupied orbital as the ferrocene- and O-based transitions; the differences in the term values may be attributed to the differences in the screening of the high-

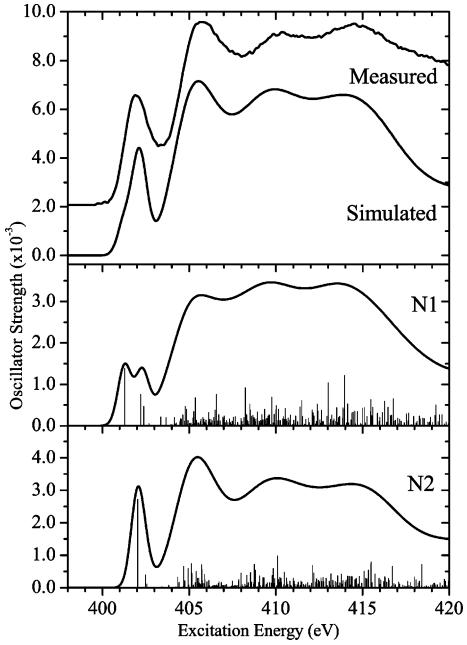

Figure 10. Simulated N 1s XAS spectra of the two nitrogen sites in Fc-Pro_2-OBz (bottom two panels) and the comparison of the total simulated N 1s XAS spectrum with the measured spectrum (top panel). The measured spectrum has had a vertical offset added for clarity.

TABLE 2: Transition Energies and Term Values of Features in Simulated O 1s XAS Spectrum

site	core level (eV)	feature (eV)	term value (eV)	assignment
O1	536.84	532.61	4.23	N/C═O π*
O1	536.84	533.63	3.21	amide σ*
O1	536.84	534.04	2.80	O/N−C σ*
O2	536.67	532.65	4.01	N/C═O π*
O2	536.67	533.55	3.11	amide σ*
O3	538.40	533.31	5.09	C═O π*
O4	539.39	535.13	4.25	C−O−C σ*

TABLE 3: Transition Energies and Term Values of Features in Simulated N 1s XAS Spectra

site	core level (eV)	feature (eV)	term value (eV)	assignment
N1	405.66	401.65 (401.3)	4.01	N/C═O π*
N1	405.66	402.59 (402.6)	3.08	amide σ*
N1	405.66	402.76 (402.4)	2.91	O/N−C σ*
N1	405.66	403.74 (403.3)	1.92	N/C−H σ*
N2	406.19	402.41 (402.0)	3.78	N/C═O π*
N2	406.19	402.87 (402.5)	3.32	amide σ*
N2	406.19	402.94 (402.5)	3.26	O/N−C σ*

energy states between the different elements. The summary of the term values and proposed assignments of the sharp features in the simulated N 1s XAS spectra is shown in Table 3. The energy values of the features correspond to the calculated values, and the values in parentheses take into account the 0.4 eV shifts that were applied to the spectra displayed in Figure 10.

The simulated and measured Fc-Pro_2-OBz spectra contain two broad features at 410.0 and 414.3 eV, the same locations as previously observed features in the N 1s XAS spectra of glycine monomers and peptides. These features had previously been attributed to EXAFS-like oscillations,[44] but this assignment seems unlikely because such a feature would not be reproduced by the current simulation. It seems, therefore, that the features must correspond to real, high-energy electronic states, or as the StoBe simulations suggest, the superposition of a large number of such states.

Fe 2p XAS. The Fe 2p XAS of Fc-COOH, Fc-$(COOH)_2$, and Fc-Pro_n-OBz series were unaffected by the type of the

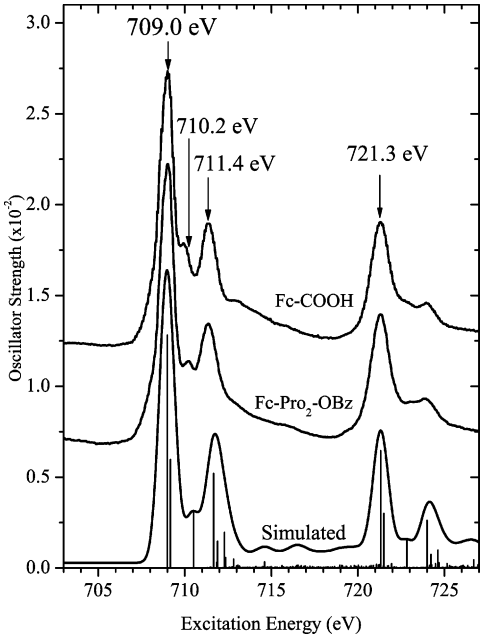

Figure 11. Measured and simulated Fe 2p XAS spectra of Fc-Pro_2-OBz and the measured spectrum of Fc-COOH. The measured spectra have had a uniform background signal subtracted, and a vertical offset was added for clarity.

substituent, except for a slight shift (~0.3 eV) in the energy of the feature around 710.2 eV. The spectrum of Fc-Pro_2-OBz is representative of the entire series of compounds; the inclusion of the measurements of Fc-Pro_n-OBz ($n = 2-4$) in Figure 11 would be redundant. Some small amount of charging may have contributed to the sloping onset of the Fe 2p XAS spectra, but this does not seem to have a significant effect on the overall spectra. The results of the StoBe simulation of the 2p XAS are also shown in Figure 11. Only the excitations originating in the $2p_{3/2}$ shell were calculated, the lower-intensity $2p_{1/2}$ feature was created by shifting the $2p_{3/2}$ feature upward by 12.3 eV and scaling it to the intensity of the measured spectrum. All transitions in the simulated spectrum were broadened by the same amount; there were convoluted with a Gaussian function of width 1.0 eV. The spectra are quite similar to previously published results of substituted ferrocenes, although the improved resolution allows the feature at 710.2 eV to be distinguished. This feature was not observed in the previous studies, and examination of the spectra suggests that this may have led to an erroneous assignment of the spectral features in the Fe 2p XAS. The two lowest-energy features are separated by 1.2 eV, identical to the separation between the portion of feature a assumed to be associated with the Cp rings and feature b in the C 1s XAS spectra (Figures 2 and 3). The 709.0 eV peak is produced by transitions from the Fe 2p levels into the $3e_{2u}$-like orbitals of the ferrocene, and it is here proposed that the 710.2 eV feature is associated with transitions into the same $4e_{1g}$-like orbitals associated with feature b in the C 1s XAS spectra. Previous publications[1,5] had associated these transitions with the prominent feature found at 711.4 eV, despite the considerable disagreement between the term value of this feature and the corresponding feature in the C 1s XAS.

The term values and proposed assignments of the features in the Fe 2p XAS spectrum are given in Table 4. As in Table 1, the values given correspond to the unshifted simulation; the spectra shown in Figure 11 were shifted approximately −3.0 eV to match up with the measured spectrum. The term values of the two lowest transitions are slightly higher than the values shown in Table 1, but the separation between them is consistent

TABLE 4: Transition Energies and Term Values of Features in Simulated Fe 2p XAS Spectrum

site	core level (eV)	feature (eV)	term value (eV)	assignment
Fe	717.73	713.03	4.70	$4e_{1g}$-like
	717.73	713.21	4.52	$4e_{1g}$-like
	717.73	714.55	3.18	$3e_{2u}$-like #1
	717.73	715.70	2.03	C−H σ*
	717.73	715.88	1.85	C−H σ*
	717.73	715.94	1.79	C−H σ*
	717.73	716.33	1.40	C−H σ*

with the separation of the transitions into $4e_{1g}$-like orbitals observed in the simulated C 1s XAS spectra, and so the main peak in the Fe 2p XAS spectra can comfortably be attributed to these transitions, in accordance with previous findings.[1,4] It is clear from the term values that, as was proposed previously, the feature seen at 710.2 eV in the Fc-Pro-OBz spectrum is associated with the $3e_{2u}$-like orbital of the substituted cyclopentadienyl (feature b in Figures 2 and 3). The oscillator strength of the transition into the other $3e_{2u}$-like state is negligible, and so it is not included in Table 4, although it should be noted that the term value of that transition is in agreement with the value given in Table 1. The small differences in term values between the Fe 2p XAS transitions and the corresponding C 1s XAS transitions is likely due to differences in the effect of the core hole on the energies of the unoccupied states. Because the $4e_{1g}$-like orbitals are closely associated with the Fe 3d state, while the $3e_{2u}$-like states have more of a C π* contribution, it seem reasonable to assume that the latter orbitals would be shifted more strongly by C core holes and that the former would be more strongly affected by Fe core holes.

The transitions that comprise the large peak at 711.4 eV involve Fe states with a large *s*-component and have term values that, in the first two cases, agree well with those of the transitions seen in the C 1s XAS, attributed to C−H σ* orbitals. This agreement, along with the presence of the $3e_{2u}$-like feature at 710.2 eV in Figure 11, suggests that the previously published[1,5] association of the 711.4 eV feature with $3e_{2u}$-like orbitals was erroneous.

Conclusions

Soft X-ray absorption spectroscopy was used to study the electronic structures of a series of novel peptide compounds, Fc-Pro_n-OBz ($n = 1-4$). The absorption spectra were simulated using StoBe DFT, and good agreement with the measured results was obtained in all cases. To our knowledge, Fc-Pro_2−OBz is the largest single molecule to have its XAS spectra successfully modeled using StoBe. The site-specific XAS simulations allowed for a clear and unequivocal assignment of the features in the measured spectra. Examination of the C 1s XAS spectra showed a break in the degeneracy of the ferrocene $3e_{2u}$-like orbitals associated with the substituted and unsubstituted Cp rings, an observation that was confirmed by the simulations. This split is not unexpected,[45] but to our knowledge, this is the first time that it has been observed experimentally. The main advantage of our results over the previously published EELS spectra is the increased resolution, which made observation of this feature possible.

Examination of the measured and simulated O 1s XAS spectra affirmed the effect of the carbonyl's environment on the energy position of the oxygen π* feature, extrapolating the previous observations of isolated carbonyl groups to apply to larger molecules with multiple carbonyl groups. Understanding of this energy dependence is shown to be a valuable tool in the interpretation of relatively complex molecular spectra. The N 1s XAS spectra also showed the effects of the extended structure on the appearance of the spectra. The StoBe simulations showed transitions into a molecular orbital having an origin that stems from the extended, rather than local, environment of the N sites.

The Fe 2p XAS spectra provided an excellent probe into the electronic structure of the substituted ferrocene. The combination of XAS and DFT was used to reassign a prominent feature in the Fe 2p XAS structure of substituted ferrocene, increasing the pool of knowledge regarding the metal−ligand interaction in organometallic molecules. This conclusion could not have been made unambiguously without the ability to compare the Fe 2p XAS results with the site-specific calculations of the ligand C 1s XAS spectra, demonstrating the utility of this sort of simulation in the analysis of the absorption spectra of relatively complex molecules.

The study of these ferrocene−peptide conjugates has increased the wealth of knowledge regarding the electronic structures of the components, information that can be used to tailor the properties of similar compounds. It is also vital to the understanding of the role of peptides in the electron transfer reactions in larger molecules. The extent of the interaction between widely separated components in a relatively large molecule has been probed, with the XAS spectra suggesting that low-lying unoccupied orbitals are somewhat delocalized throughout the structure. This information may be used to develop piecemeal models of peptides in very complex systems. It is clear that the XAS spectra of a system of interacting prolines cannot be completely modeled as being summations of the spectra of the individual residues, and it is reasonable to expect that this conclusion can be generalized to other amino acids. If the XAS spectra of proteins are to be analyzed using a building block approach, our results suggest that the spectra of peptides, rather than individual amino acids, must be used to this end, specifically if the N and O 1s XAS are being examined.

Acknowledgment. Funding by the Natural Sciences and Engineering Research Council of Canada (NSERC), the Saskatchewan Synchrotron Institute, and the Canada Research Chair program is gratefully acknowledged. The work at the Advanced Light Source was supported by the U.S. Department of Energy (Contract DE-AC03-76SF00098). R.G.W. thanks John Tse (University of Saskatchewan) and Lars Pettersson (Stockholm University) for their guidance in regards to the DFT calculations.

References and Notes

(1) Wen, A. T.; Ruhl, E.; Hitchcock, A. P. *Organometallics* **1992**, *11*, 2559.

(2) Ruhl, E.; Heinzel, C.; Baumgartel, H.; Hitchcock, A. P. *Chem. Phys.* **1993**, *169*, 243.

(3) Ruhl, E.; Hitchcock, A. P. *J. Am. Chem. Soc.* **1989**, *111*, 5069.

(4) Hitchcock, A. P.; Wen, A. T.; Ruhl, E. *Chem. Phys.* **1990**, *147*, 51.

(5) Hitchcock, A. P.; Wen, A. T.; Ruhl, E. *J. Electron Spectrosc.* **1990**, *51*, 653.

(6) Getty, S. A.; Engtrakul, C.; Wang, L.; Liu, R.; Ke, S. H.; Baranger, H. U.; Yang, W.; Fuhrer, M. S.; Sita, L. R. *Phys. Rev. B* **2005**, *71*, 241401.

(7) Boese, J.; Osanna, A.; Jacobsen, C.; Kirz, J. *J. Electron Spectrosc.***1997**, *85*, 9.

(8) Carravetta, V.; Plashkevych, O.; Agren, H. *J. Chem. Phys.***1998**, *109*, 1456.

(9) Kaznacheev, K.; Osanna, A.; Jacobsen, C.; Plashkevych, O.; Vahtras, O.; Agren, H. *J. Phys. Chem. A* **2002**, *106*, 3153.

(10) Tanaka, M.; Nakagawa, K.; Koketsu, T.; Agui, A.; Yokoya, A. *J. Synchrotron Radiat.* **2001**, *8*, 1009.

(11) Tzvetkov, G.; Koller, G.; Zubavichus, Y.; Fuchs, O.; Casu, M. B.; Heske, C.; Umbach, E.; Grunze, M.; Ramsey, M. G.; Netzer, F. P. *Langmuir* **2004**, *20*, 10551.

(12) Gordon, M. L.; Cooper, G.; Morin, C.; Araki, T.; Turci, C. C.; Kaznatcheev, K.; Hitchcock, A. P. *J. Phys. Chem. A* **2003**, *107*, 6144.

(13) Cooper, G.; Gordon, M.; Tulumello, D.; Turci, C.; Kaznatcheev, K.; Hitchcock, A. R. *J. Electron Spectrosc.* **2004**, *137*−*40*, 795.
(14) Kraatz, H.-B.; Leek, D. M.; Houmam, A.; Enright, G. D.; Lusztyk, J.; Wayner, D. D. M. *J. Organomet. Chem.* **1999**, *589*, 38.
(15) Plashkevych, O.; Carravetta, V.; Vahtras, O.; Agren, H. *Chem. Phys.* **1998**, *232*, 49.
(16) Yang, L.; Plashkevych, O.; Vahtras, O.; Carravetta, V.; Agren, H. *J. Synchrotron Radiat.* **1999**, *6*, 708.
(17) Messer, B. M.; Cappa, C. D.; Smith, J. D.; Wilson, K. R.; Gilles, M. K.; Cohen, R. C.; Saykally, R. J. *J. Phys. Chem. B* **2005**, *109*, 5375.
(18) Messer, B.; Cappa, C.; Smith, J.; Drisdell, W.; Schwartz, C.; Cohen, R.; Saykally, R. *J. Phys. Chem. B* **2005**, *109*, 21640.
(19) Nyberg, M.; Hasselström, J.; Karis, O.; Wassdahl, N.; Weinelt, M.; Nilsson, A.; Pettersson, L. G. M. *J. Chem. Phys.* **2000**, *112*, 5420.
(20) Nyberg, M.; Odelius, M.; Nilsson, A.; Pettersson, L. G. M. *J. Chem. Phys.* **2003**, *119*, 12577.
(21) Hasselström, J.; Karis, O.; Nyberg, M.; Pettersson, L. G. M.; Weinelt, M.; Wassdahl, N.; Nilsson, A. *J. Phys. Chem. B* **2000**, *104*, 11480.
(22) Hasselström, J.; Karis, O.; Weinelt, M.; Wassdahl, N.; Nilsson, A.; Nyberg, M.; Pettersson, L. G. M.; Samant, M. G.; Stöhr, J. *Surf. Sci.* **1998**, *407*, 221.
(23) Zubavichus, Y.; Shaporenko, A.; Grunze, M.; Zharnikov, M. *J. Phys. Chem. A* **2005**, *109*, 6998.
(24) Zubavichus, Y.; Fuchs, O.; Weinhardt, L.; Heske, C.; Umbach, E.; Denlinger, J. D.; Grunze, M. *Radiat. Res.* **2004**, *161*, 346.
(25) Zubavichus, Y.; Zharnikov, M.; Shaporenko, A.; Fuchs, O.; Weinhardt, L.; Heske, C.; Umbach, E.; Denlinger, J. D.; Grunze, M. *J. Phys. Chem. A* **2004**, *108*, 4557.
(26) Xu, Y. M.; Saweczko, P.; Kraatz, H.-B. *J. Organomet. Chem.* **2001**, *637*, 335.
(27) MacNaughton, J. B.; Moewes, A.; Kurmaev, E. Z. *J. Phys. Chem. B* **2005**, *109*, 7749.
(28) Underwood, J. H.; Gullikson, E. M. *J. Electron Spectrosc.* **1998**, *92*, 265.
(29) Underwood, J. H.; Gullikson, E. M.; Koike, M.; Batson, P. J.; Denham, P. E.; Franck, K. D.; Tackaberry, R. E.; Steele, W. F. *Rev. Sci. Inst.* **1996**, *67*, 3372.
(30) Kaznacheyev, K.; Osanna, A.; Jacobsen, C.; Plashkevych, O.; Vahtras, O.; Agren, H. *J. Phys. Chem. A* **2002**, *106*, 3153.
(31) Moewes, A.; MacNaughton, J.; Wilks, R.; Lee, J. S.; Wettig, S. D.; Kraatz, H.-B.; Kurmaev, E. Z. *J. Electron Spectrosc.* **2004**, *137*−*40*, 817.
(32) Augustsson, A.; Herstedt, M.; Guo, J. H.; Edstrom, K.; Zhuang, G. V.; Ross, P. N.; Rubensson, J. E.; Nordgren, J. *Phys. Chem. Chem. Phys.* **2004**, *6*, 4185.
(33) Fomichev, V. A.; Rumsh, M. A. *J. Phys. Chem. Sol.* **1968**, *29*, 1015.
(34) Lusvardi, V. S.; Barteau, M. A.; Chen, J. G.; Eng, J.; Fruhberger, B.; Teplyakov, A. *Surf. Sci.* **1998**, *397*, 237.
(35) Hermann, K.; Pettersson, L. G. M.; Casida, M. E.; Daul, C.; Goursot, A.; Koester, A.; Proynov, E.; St.-Amant, A.; Salahub, D. R. Contributing authors: Carravetta, V.; Duarte, H.; Friedrich, C.; Godbout, N.; Guan, J.; Jamorski, C.; Leboeuf, M.; Leetmaa, M.; Nyberg, M.; Pedocchi, L.; Sim, F.; Triguero, L.; Vela, A. *Stobe Software*; StoBe-DeMon Version 2.1, 2005.
(36) Kraatz, H.-B.; Lusztyk, J.; Enright, G. D. *Inorg. Chem.* **1997**, *36*, 2400.
(37) Hermann, K.; Pettersson, L. *Documentation for StoBe2005*, Version 2.1, 2005, http://w3.rz-berlin.mpg.de/∼hermann/StoBe/StoBeMAN.html.
(38) Kutzelnigg, W.; Fleischer, U.; Shindler, M. In *NMR*−*Basic Principles and Progress*; Springer-Verlag: New York, 1990; Vol. 23, p 165.
(39) Hitchcock, A. P.; Fischer, P.; Gedanken, A.; Robin, M. B. *J. Phys. Chem.* **1987**, *91*, 531.
(40) Urquhart, S. G.; Ade, H. *J. Phys. Chem. B* **2002**, *106*, 8531.
(41) Puttner, R.; Kolczewski, C.; Martins, M.; Schlachter, A.; Snell, G.; Sant'anna, M.; Viefhaus, J.; Hermann, K.; Kaindl, G. *Chem. Phys. Lett.* **2004**, *393*, 361.
(42) Francis, J. T.; Hitchcock, A. P. *J. Phys. Chem.* **1992**, *96*, 6598.
(43) Püttner, R.; Kolczewski, C.; Martins, M.; Schlachter, A. S.; Snell, G.; Sant'anna, M.; Viefhaus, J.; Hermann, K.; Kaindl, G. *Chem. Phys. Lett.* **2004**, *393*, 361.
(44) Zubavichus, Y.; Zharnikov, M.; Schaporenko, A.; Grunze, M. *J. Electron Spectrosc.* **2004**, *134*, 25.
(45) Dowben, P. A.; Driscoll, D. C.; Tate, R. S.; Boag, N. M. *Organometallics* **1988**, *7*, 305.